ORIGINAL ARTICLE

Modulating effect of graphine oxide loaded hesperidin nanocomposite on the 1,2-dimethylhydrazine provoked colon carcinogenesis in rats via inhibiting the iNOS and COX-2 pathways

Jin Liu [a], Xiaoyan Ma [b], LingWang [c],*

[a] *Department of Oncology, Affiliated Hospital of Weifang Medical University, Weifang, Shandong 261031, China*
[b] *Department of Critical Medicine, Weifang People's Hospital, Weifang ,Shandong 261041, China*
[c] *Medical Experimental Training Center, Weifang Medical University, Weifang, Shandong 261053, China*

Abstract Hesperidin is a flavonoid derived from citrus plant peels. It have convinced biological actions, which includes antioxidant possessions, anti-inflammatory outcome, and thus we investigate that hesperidin will encompass chemopreventive probable next to 1,2-dimethylhydrazine (DMH)-provoked experimental colon carcinogenesis in male Wistar rats. Rats were randomly alienated into six groups. Group I rats were considered as control. Group II rats received only DMH. Groups III&IV animals received 20 mg/kg b.w of DMH subcutaneous one time a week, for initial 4 weeks. In adding, groups III & IV animals given DMH along with hesperidin at the dose of 5&10 mg/kg b.w., correspondingly for about 16 weeks. In present study we optimized hesperidin loaded with graphine oxide as a result achieved and was itemized and illustrated by UV Visible spectroscopy (876.25 nm), X-Ray diffraction, Fourier Transform Infrared Spectroscopy and Dynamic light scattering (45.50 nm). Hesperidin to the DMH induced rats drastically diminished the incidence of polyps as contrast to the DMH alone animals. Additionally in hesperidin management over DMH exposed experimental rats, we observed elevated actions of the oxidation inhibitors and diminished planes of LPO in liver and passage along with improved stage of lipids and antioxidants in colon tissues, which be distorted in the DMH unaided rats. Moreover, we experiential tainted actions of Interleukins, tumor necrosis factor and bioactive enzymes in DMH only rats,

* Corresponding author at: Medical Experimental Training Center, Weifang Medical University, Weifang, Shandong 261053, China.
E-mail address: lingwang73@sina.com (LingWang).
Peer review under responsibility of King Saud University.

Production and hosting by Elsevier

which are upturned in hesperidin treatment. All remarks are sustained in our histological conclusion. Ultimately, hesperidin might worned as effectual chemopreventive agent adjacent to DMH tempted colon cancer.

1. Introduction

Colon cancer is the third utmost common cancer in both genders with roughly around 695,000 documented mortalities from the disease in 2012 globally (Globocan, 2012). In current years, augmented amount of recounted individuals of colon cancer have prepared this type of tumor a foremost wellbeing apprehension (Siegel et al., 2014). The speed of colon cancer is aggregating due to the extreme alteration in the nutritional array. Global epidemiologic educations displayed an interaction between nutrition and the occurrence of gastrointestinal tract cancer, particularly colon cancer, which can be endorsed by an ironic diet in meat and high fat (Siegel et al., 2014). Numerous revisions as well as many recent and preceding studies have shown that an extraordinary fat regime encourages tumorigenesis in the chemical induced investigational animal models of colon carcinogenesis (Sangeetha et al., 2012; Aranganathan et al., 2009; El-Khadragy et al., 2018). The surgical procedure and administration of chemotherapeutic drugs are the primary choices for the treatment of colon cancer (Xiong and Xiao, 2018). However, the increased side effects of these approaches often experienced by the colon cancer patients. These side effects are restricts the utilization of these treatment approaches. Hence there is a huge need for the development of herbal based drugs with the very minimal side effects (Twelves et al., 2005).

DMH (1, 2- Dimethylhydrazine) an effective procarcinogen displaying discernment on the road to the colon cancer, was used in present study. This exemplary display that DMH persuades rat colon carcinogenesis duplicates humanoid colonic epithelial abnormal growth of tissue in its anatomy and histology (Juan et al., 2019). It has extensively promoted to tempt colon carcinogenesis in rodent species (Liu et al., 2018; Sugihara et al., 2017). DMH, a metabolic prototype of MAM (methylazoxy methanol), which entails metabolic initiation to further customize DNA combative products. Principally, DMH is processed to formazoxymethane, which is additionally processed to give MAM through P4502E1 cytochrome in liver with preceding work by Megaraj et al. (2014). Methylazoxy methanol gets accusative in the liver by glucuronic acid and it is discharged to the colon through blood or bile as methylazoxy methanol glucuronide where it is unconjugated by activities of gastrointestinal bacterial enzymes specially β-glucuronidase toward produce methylazoxy methanol (Sun et al., 2019). The renewed MAM is supplementary processed to give rise to electrophilic species of methyldiazonium ion, which sequentially produces carbonium ion that is accountable for the addition of methyl group of nucleic acids and turns as an initiator for colon cancer (Rosenberg et al., 2009). An abnormal crypt focus (ACF) has been considered as the antecedent of colon cancer (Rudolph et al., 2005; Bird and Good, 2000; Mori et al., 2005). ACF has been broadly used as a primary biomarker and is supposed to be a substitute preneoplastic scratch subsequently it is established in the colon carcinogen of preserved rodents and humans. They are effortlessly visual under microscope (light) by formulating a formalin immovable methylene blue discolored complete mount mucosal colon tissues. Chemical, hereditary and structures revisions exposed and colon cancers stake similar modifications (Rudolph et al., 2005).

Nano materials as medicine transporters have developed a hot plug for investigation at the boundary of nanotechnology and biology since they permit effectual packing, embattled distribution, and sustained discharge of drugs. They are capable apparatus in modern rehabilitation of cancer as they diminish the hazard of adverse effects and multidrug confrontation in tumor cells (Biju, 2014; Venkatraman et al., 2012). A diversity of nanomaterials, such as grapheme some of the noble metals like silver, gold nanoparticles, natural polymers, and nanoparticles of liposome, with diverse shape and alteration of their exterior have been amalgamated and accounted to have objective précised and improved anti-tumor action (Senapati et al., 2018; Malmsten, 2013; Al Faraj et al., 2016).

Products from natural with assorted pharmacological possessions have expanded robust consideration in the hindrance and management of innumerable illnesses counting cancer. A huge quantity of phytochemicals has been appraised as of the nutrition as well therapeutic vegetation for anti-tumor commotion owing to extraordinary capability to hinder amid numerous passageway governing development and death of cancer cells. Horticulture crops include fruits, vegetables and grapes very rich for phytochemicals and have been indicated to be responsible for this observed protective effect against cancer. Thus it is promoting higher consumption of these health-promoting substances (Zia-Ul-Haq et al., 2014; Marsic et al., 2019; Senica et al., 2019; Gecer et al., 2020). In the middle of the flavonoids, Hesperidin a citrus flavonoid has lately occurred as an exclusive cluster of phytochemical with high performance biological activities. Hesperidin possesses numerous pharmacological properties like cardioprotection (Trivedi et al., 2011), anti-inflammatory (Parhiz et al., 2015), anti-oxidant (Parhiz et al., 2015), anti-diabetes (Bai et al., 2019), anticancer (Tanaka et al., 2012), and neuroprotection (Jo et al., 2019). Hesperidin has exposed anti-cancer actions, though the later displayed developed antiproliferative commotion in vitro studies (Chen et al., 2003). Furthermore, hesperidin has been stated it subdues propagation of both human breast and androgen reliant prostate cancer cells (Lee et al., 2010). Promising consequences animal study carcinogenesis reticence by hesperidin has correspondingly experiential. Hesperidin was established to constrain 4-NQO persuaded oral carcinogenesis and to diminution the quantity of abrasions, polyamine intensities in tissue of tongue, and cell explosion movement (Tanaka et al., 1994). Furthermore, when hesperidin managed intravenously to CD-1 mice, it reserved tetradecanoylphorbol-13-acetate induced tumor

preferment in mouse skin carcinogenesis (Berkarda et al., 1998). Interestingly preceding study shows that hesperitin, an aglycoside, minute structurally altered compound from hesperidin at a dose of 20 mg/kg body weight for 15 weeks reserved colon cancer in rat model (Aranganathan et al., 2009). The amazing biological properties of hesperidin engrossed our consideration to theorize the current study that hesperidin will have protective possessions on DMH empted rat colon cancer. In present study we appraise the potential of hesperidin on oxidative trauma markers, biotransforming enzymes, in DMH-induced experimental rat colon carcinogenesis through inhibiting iNOs and COX-2 pathway.

2. Materials and methods

2.1. Chemicals

1,2-dimethylhydrazine (DMH) and Hesperidin be procured from Sigma chemical (Missouri, United States). Other reagents plus chemicals are investigative rank, acquired from HiMedia Biosciences, USA. Thiobarbituric acid reactive substances, Sodium Oxide Dismutase, Catalase, NADH, NADP, INOS, COX-2, Caspase- 3&9, IL-6, IL-1β and TNF-α (ELISA) were purchased from GeneTex (California, United States). Goat anti-rabbit immunoglobulin G (IgG) secondary antibody and peroxidase were purchase from Abcam (Cambridge, United Kingdom).

2.2. Preparation of graphine oxide

The graphine oxide nanosheets with the thickness of less than 2 nm, on the side size ~110–800 nm, and mean width was about 450 nm were equipped and distinguished as portrayed (Chen et al., 2014, 2012) and detached in water at 200 μg/mL as the stock solution. The facts for graphine oxide nanosheets amalgamation and categorization are explained in accompanying substance.

2.3. Experimental animals

Wistar rats (male albino 4–8 weeks aged) weighing 125–145 g be attained as well sustained for investigational studies next to Institutional Animal Care and Committee of Taipei Medical University, Taiwan. The rats were concerned in conformity with ethics and guiding principle of Taipei Medical University. Animals were nurtured in a disinfected seat of husk in polypropylene cages with pathogen liberated animal room by prohibited circumstances of 12 hr light/12 hr dark cycle, with warmth of 22 °C and comparative dampness of 50% till the experimental duration. Wistar rats were fed through a standard pellet (Hindustan, Mumbai, India). All through the investigational period, pellet diet and water be fed ad libitum.

2.4. Experimental design

Rats were randomly divided into six experimental groups of six rats each; then they were quarantined for 2 weeks for environmental and trainer handling acclimatization before initiation of the experiment. Group I rats received modified diet for 16 weeks and served as controls. Groups II–IV rats received modified diet with subcutaneous injections of DMH (20 mg/kg bw) once a week, for the first 4 weeks. In addition, groups III–IV rats received different doses of Nps orally every day (5 and 10 mg/kg bw, respectively) along with the modified pellet diet and DMH injections.

2.5. Hesperidin preparation

Hesperidin was dissolved in the 5% of dimethyl sulfoxide (DMSO) (Ramachandran and Saravanan, 2013) prior to the handling and be managed orally daily at the dose of 5 and 10 mg/kg b.w right through the experimental phase.

2.6. Devising of carcinogen management

DMH was liquefied in 1 mM EDTA immediately before start of the experiment and pH was accustomed to 6.5 by 1 mM NaOH, toward safeguarding constancy of carcinogen. Then the carcinogen administered (subcutaneously) in the thigh (right) at 20 mg/kg b.w one time a week, for the initial a month of the examination (Aranganathan et al., 2009).

2.7. UV–Visible spectroscopy examination

The deterioration of unblemished graphine oxide was recognized by influentially with the amalgamation of rejoinder assortment by UV Visible Spectrophotometer from 350 to 800 nm (Chattopadhyay et al., 2013; Ghantoji et al., 2015).

2.8. X-ray diffraction analysis

To determine the attractiveness and size of the graphine oxide nanoparticles, X-ray diffraction (XRD) was performed. The sample pellets was deferred in deionized water and the scrubbing procedure recurrent for 3 times by the similar solution shadowed by centrifugation. The pellet was conserved and allowable to dry. The residue instigating from the sample was enclosed on the XRD network, the spectra were recognized 40 kV and a current of 30 mA with alpha and beta radiation through XRD (PW1050, Philips). The thinned strengths were confirmed from 22 to 85 °C at 2 theta angles. The sparkling atmosphere of merged nanoparticles was intended from the range of the XRD peak, by standard formula (Debye-Scherrer) (Tensingh Baliah and Lega, 2018).

2.9. Dynamic light scattering analysis

To determine the particle dimensionby dynamic light scattering (DLS), we use the method developed by Kumar and Münstedt (2005). In which 0.01gm of polymer powder includes 12 mmol silver nitrate extorted in 20 ml distilled.

2.10. Fourier Transform Infrared (FTIR) analysis

FTIR has been rehabilitated into a substantial device for the contemplation of the influence of functional groups in transportations between metal particles and organic molecules. FTIR spectra were confirmed at 1 cm^{-1} signal by FTIR

spectrophotometer (FT-IR-6800JASCO Europe) using Potassium Bromide pellet process (Patra et al., 2011). The incidence display was reflected as wave facts habitually over the range 4000–400 cm^{-1}.

2.11. Body mass and growth proportion alterations

Throughout the investigational period for about 4 months, body mass and expansion rate of the normal and experimental animals were evaluated. The experimental animals were considered proceeding to experimentation, consequently formerly each week and lastly prior to detriment.

2.12. Occurrence of abnormal stalks or polyps and its evaluation

At the termination of the investigational epoch, animals were forfeited and colonic mucosa was detached also blushed with biological saline. The mucosal colons were cut unwrap measurably not troubling the polyps and cautiously calculated by means of visual macroscopic inspection and later confirmed with histological studies.

2.13. Preparation of tissue and plasma samples

After the experimentation is completed i.e. about four months, rats were surrendered beneath anesthesia (i.p.) by the directed use of ketamine hydrochloride, 30 mg/kg body weight by cervical amputation subsequently an instantaneous fasting. Instantaneously following to forfeit, liver, distal and proximal colonic stuffs were scrutinized, cleansed in saline. Colonic stuffs were crushed and homogenized in appropriate buffer using a tissue grinder, and then centrifuged for about 15 min at 1200g at 4 °C. Resultant precipitation was selected for assays like biochemical studies.

Blood samples were unruffled in heparin coated hose and the plasma was alienated through centrifuging for about 10 min at 2000g. Following partition of plasma, the yellowish coat was detached and crowded red blood cells (RBC) were 3 times rinsed in cold saline. Erythrocyte lysate was equipped as a result of lysis of an identified quantity of red blood cells among hypotonic phosphate solution of buffer, at pH 7.4. Lysate was subsequently alienated next to centrifugation for 15 min at 3000g at 4 °C.

2.14. Assessment of oxidative deprivation of lipids

Lipid peroxidation was deliberated by ascertaining the light intensity (spectrophotometry) point of the tissue lipid peroxidation secondary products. TBARS (Thiobarbituric acid reactive substances) were predictable through the Ohkawa et al. (1979) methods and further subsequently the lipid hydroperoxides (LOOH) by the process of Jiang et al. (1992) and conclusively conjugated dienes (CD) determined by the system of Ra and Recknagel (1968).

2.15. Determination of antioxidants level

Superoxide dismutase (SOD) was examined by the technique of Kakkar et al. (1984) and catalase (CAT) assay was executed by Sinha (1972). Reduced glutathione (GSH) was resolute by Ellman method (1959) glutathione peroxidase (GPx) levels were scrutinized by the technique of Rotruck et al. (1973) and ultimately glutathione reductase (GR) measurement was done by Carlberg and Mannervik (1985).

2.16. Inference of phase I&II enzymes

Cytochrome P450 was considered by the process of Omura and Sato (1964) and Cytochrome 4502E1 inference was done by the protocol of Watt et al. (1997)). GST was assessed by the means of Habig et al. (1974). Protagonist of NADPH-Cytochrome P450 Reductase, Cytochrome-b5 and NADPH-Cytochrome b5 Reductase inference was done by protocol (Gan et al., 2009).

2.17. Immunohistochemical analysis

Segment of 4 μm were censored from formalin immobile, paraffin entrenched tissue chunks and attached on lysine covered microscopic slithers. The procedure charted it was rendering to Ahmed et al. (2016). Paraffinized segments were dewaxed in xylene and rehydrated by ordered sequences of ethanol to water trailed by antigen repossession in sodium citrate buffer (10 mM) at pH 6.0. The slips were permissible to cool for 20 min and washed 3 times with tris-buffered saline (TBS) for 5 min. Slithers are nurtured in hydrogen peroxide (3%) in methanol for 15 min to lessen the inner peroxidase action and then mattered to Ultra wedge (Ultra Vision, LPDetection, Thermo Scientific) for about 15 min to lump nonspecific obligatory. The slides were kept overnight at 4 °C with primary antibody along with humidified compartment and then pounded in TBS. The sections were gestated with goat anti-polyvalent secondary antibody for 20 min and then were rinsed in TBS, this step was repeated again. Later washed in TBS and settled with 3, 3′-Diaminobenzidine (DAB) solution till segments developed in brown color. Then counter stamp the segments with Mayer's haematoxylin, equestrian by mounting media and then examined under the light microscope (Olympus BX43).

2.18. Assay of pro-inflammatory markers level

Tumor necrosis factor-α (TNF-α), interleukin-6 (IL-6) and interleukin-1β (IL-1β) protein level was measured by enzyme-linked immunosorbent assay (ELISA) kit (Ebioscience, Incorporation California USA). Investigation was accomplished rendering to themanufacturer's protocol.

2.19. Histopathological examination

Histological investigation was achieved to perceive any extreme modifications have been observed. A ration of the liver and colon mucosa tissues from dissimilar clusters were immobile in unbiased buffered formalin (10%) for 7 days at room temperature. Liver or colon specimen was then desiccated by transient via dissimilar categorized sequence of ethyl alcohol, unfurnished in xylene and entrenched in paraffin wax (Siddique et al., 2017). Tissue lumps were then partitioned and managed using repetitive histological approaches shadowed by

H&E (haematoxylin and eosin) staining. Discolored segments were observed under (Leitz Labor) differentiating microscope and alterations were renowned.

2.20. Statistical analysis

The outcomes were approved as indicate ± SD of six rats for each cluster. The statistics were inspected by analysis of variance (ANOVA) and slightly noteworthy alterations amongst treatment clusters were appraised by means of DMRT (Duncan's multiple range test). The statistically substantial on $p < 0.05$. All arithmetical evaluates were achieved by SPSS software version 20.0 (Asia analytics, China).

3. Results

3.1. Outcome of hesperidin on animal body mass and changes in expansion rate

During experimentation phase, inconstant variations were experiential in the body mass and growth proportion of animals between the dissimilar groups (Table 1). DMH-alone-vulnerable rats (group II) displayed abridged weight gain as matched to the control. Nevertheless, the weight loss was prohibited meaning fully ($p < 0.05$) on supplementation of hesperidin with dissimilar doses (5 and 10 mg/kg b.w.) of hesperidin to DMH-liable animals.

Growth proportion was calculated as the alteration among the initial and final body mass alienated by the quantity of days. Enlargement pace was augmented pointedly on supplementation with diverse doses (5 and 10 mg/kg b.w.) of hesperidin to DMH rats (group's I–VI) as associated to the DMH-alone animals (group II). Hesperidin at the dose of 10 mg/kg b.w. expressively exposed the optimal enhanced weight improvement and growth frequency thus contributing extreme fortification to animals alongside DMH-provoked colon cancer.

3.2. Consequence of hesperidin and DMH on stalks or polyps incidence

In DMH unaccompanied animals (group II), 100% occurrence of abnormal tissue or polyps was originated (Table 2). On management by means of dissimilar dose of hesperidin (5 & 10 mg/kgb.w.) toward DMH liable rats (I–IV groups) the frequency of polyps be expressively ($p < 0.05$) condensed since associated to DMH unaided animals (cluster II). No definite alterations were discerned among control rats. When compared to 5 mg, 10 mg/kg b.w. hesperidin was originated to be added operative or effectual, over the occurrence of polyps being 67% inhibited. Average numbers of polyps also reduced from 2.79 to 1.48 (DMH to 10 mg hesperidin).

3.3. Effect of hesperidin on lipid peroxidation

Fig. 5 shows possessions of hesperidin as well DMH on the attentiveness of lipid peroxidation secondary products in the tissues of normal and experimental rats. In DMH alone animals, deliberation of TBARS was expressively ($p < 0.05$) high projecting in the blood passage and liver, however in proximal and distal colon, the deliberations were suggestively downregulated ($p < 0.05$) as comparable to control animals (group I). At the same time supplementation by means of hesperidin at the dose of 5 as well 10 mg/kg b.w. correspondingly to the DMH bared rats (III & IV), consideration of lipid peroxidation were regenerated to normal level as associated to the control rats.

3.4. Consequence of hesperidin on antioxidant events

The accomplishments of hesperidin on SOD, CAT, were suggestively ($p < 0.05$) downregulated in the liver, proximal colon and distal colon of DMH-alone-treated rats (group II) as compared to the control rats (group I). Figs. 6 and 7 displays that accretion ($p < 0.05$) with hesperidin at the dose of 5 along with 10 mg/kg b.w. toward DMH treated rats (III & IV groups) considerably elevated the accomplishments adjacent to control animals.

3.5. Outcome of hesperidin on phase I biological enzymes

The events of phase I biological enzymes like CYP450, CYP2E1, NADPH-cytochrome P450 reductase and NADH-cytochrome b5 reductase) in the liver of control and experimental animals are portrayed in Fig. 8. In the DMH alone animals (group II) the activities of NADPH-cytochrome P450 reductase, NADH-cytochrome b5 reductase, CYP450 and CYP2E1 were expressively raised as equated to the control animals (group I) while additive with hesperidin at the doses of 5 and 10 mg/kg b.w. ominously ($p < 0.05$) reduced the actions of the phase I enzymes.

3.6. Characterization results by UV–Vis, XRD, DLS and FTIR

UV–Vis spectra documented at dissimilar time period for the response with chloroauric acid resolution illustrate a primary augment in the absorbance, which later on diminished with elevated incubation epoch and become steady generous a maximum absorbance at 876.25 nm at one hour period of incubation. The manifestation of the lesser color confirms the configuration of graphine oxide nanosheets in the reaction mixture (Fig. 1). Tinted solution permitted determining the absorbance alongside dissimilar wavelength to verify the

Table 1 Initial and final body weight changes and growth rate of control and experimental groups of rats.

Groups	Initial body weight (gm)	Final body weight (gm)	Weight gain (gm)	Growth rate (gm)
Group I	143.34 ± 12.90	239.56 ± 21.56	96.22 ± 8.63	0.86 ± 0.08
Group II	145.15 ± 13.06	195.79 ± 17.61	50.64 ± 4.56	0.45 ± 0.04
Group III	146.37 ± 13.17	218.00 ± 19.61	71.63 ± 6.46	0.64 ± 0.06
Group IV	144.91 ± 13.94	236.22 ± 21.25	91.31 ± 8.20	0.82 ± 0.07

Table 2 Effect of hesperidin on the incidence of colonic polyps.

Groups	No. of polyp bearing rats	Total number of polyps	Incidence of polyps (%)	Inhibition of polyps (%)	Average numberof polyps/polyp bearing rat
Group I	Nil	Nil	Nil	–	–
Group II	6	15	100	0	2.79
Group III	4	8	60	40%	2.05
Group IV	2	3	33	67%	1.48
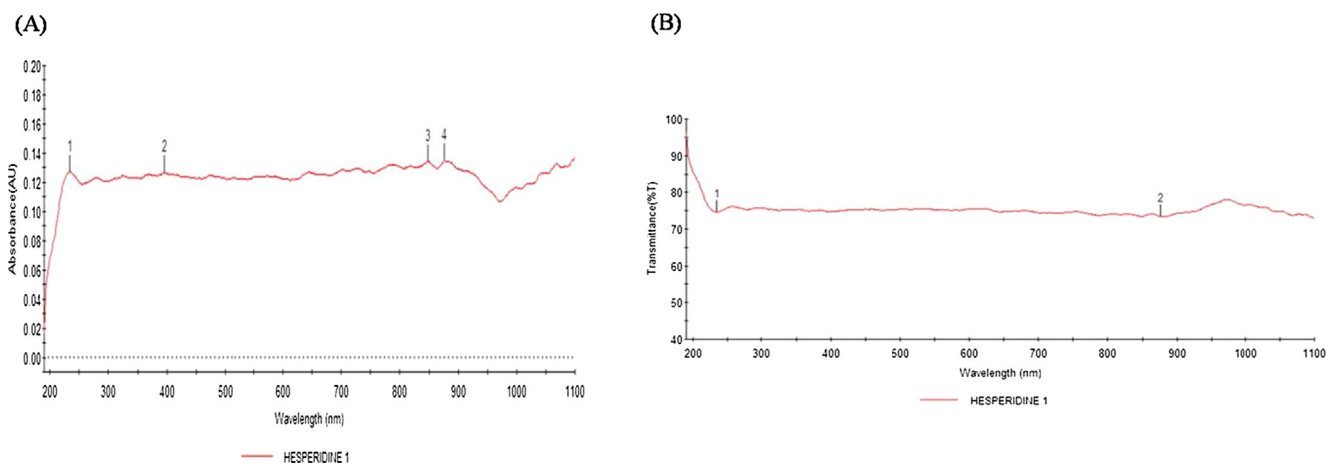
Fig. 1 UV–visible spectrum absorption pattern of graphine oxide loadsynthesised from hesperidin. UV–VIS absorption spectra of graphine oxide nanosheets. The peak values for UV–VIS, plotted between graphine oxide/absorbance ratios. The highest absorbance peak is about 876.25. All solutions were in water. (A) shows the all four absorbance values. (B) shows the optimum and highest peak absorbance of hesperidin.

development of graphine oxide nanosheets. UV–vis spectra evidenced at diverse time space for the retort with solution displayed manifestation of peak absorbance at 876.25 nm at the wavelength of 400. The corresponding UV–vis spectra recorded from hyaluronic acid diminution at different time gap is shown in Fig. 1. On decline of hyaluronic acid for a variety of instance depicted a decline in the strength of graphine oxide at 876.25 & 234.15 nm and emergence of absorbance band at 876.25 nm. No noteworthy alteration in the concentration from spectrum also recommends that the decline is over up to 980 nm wavelength.

Dynamic light scattering (DLS) is a method used to resolve the dimension, size allocation contour and polydisparity indicator of particles in a suspension. Fig. 4 shows the particle size of the nanosheets samples. After analyzing data, it was found that graphine oxide size were in the range of 100 nm. The maximum portion of graphine oxide present in the solution was of 45.50 nm.

XRD investigation, the XRD prototypes illustrate the fabrication of graphine oxide nanosheets by the reduction hyaluronic acid. The exergonic intensities have been documented from 20° to 80° by the side of 2 theta angles. The absorptive pattern depicted in Fig. 2 appreciably corresponds to graphine oxide. In the spectrum apparent peaks are not experiential it designate that thenanoparticles had a sphere-shaped configuration.

The FTIR spectra of graphine oxide loaded hesperidin with absorption peaks at 3440, 2922, 2853, 2091, 1630, 1570, 1459, 1383, 1100, 668.01 and 605.88 (cm^{-1}) were pragmatic in Fig. 3. The spectra attained to distinguish the interface between Chloroauric acid and hesperidin has strong peak at 3440.0 illustrate the OH group (widen H bonded, strapping broad) all along with the beyond peaks, few extra peaks at 2922 and 2853 were as well observed which match up to C—H group (extend strong), C—H group (changeable), C—O group (strapping), =C—H group (well-built), C=C group (unpredictable). The utmost assimilation peak at 3440 replicates the OH group may be accountable for the tumbling possessions of the hesperidin.

3.7. Result of hesperidin on pro-inflammatory markers and caspases level

We have evaluated the upshot hesperidin on DMH induced unusual upsurge in TNF-α, IL-6 and IL-1β protein level (Fig. 9). We noticed that there was a noteworthy amplification in the level of proinflammatory cytokines and interleukins 6 and 1β in DMH alone (group II) related with normal (group I). Management with hesperidin at a dose of 5 and 10 mg/kg b.wt expressively impede their anomalous proliferation in the group III & IV when contrast with DMH alone (group II) administered animals. Hesperidin at
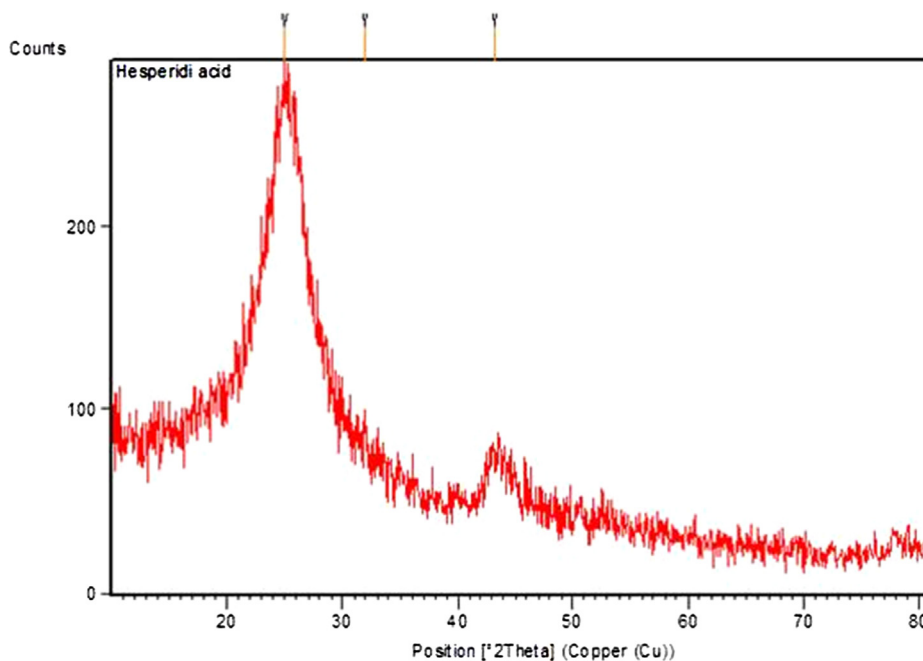
Fig. 2 X-Ray Diffraction analysis of graphine oxide nanosheetsamalgamated from hesperidin. XRD prototype illustrate the fabrication of graphine oxide by the reduction of hyaluronic acid using Hesperidin. The diffracted intensities have been evidenced from 20° to 80° at 2 theta angles. The diffracted pattern is depicted in (Fig. 2) considerably match up to untainted graphine oxide.
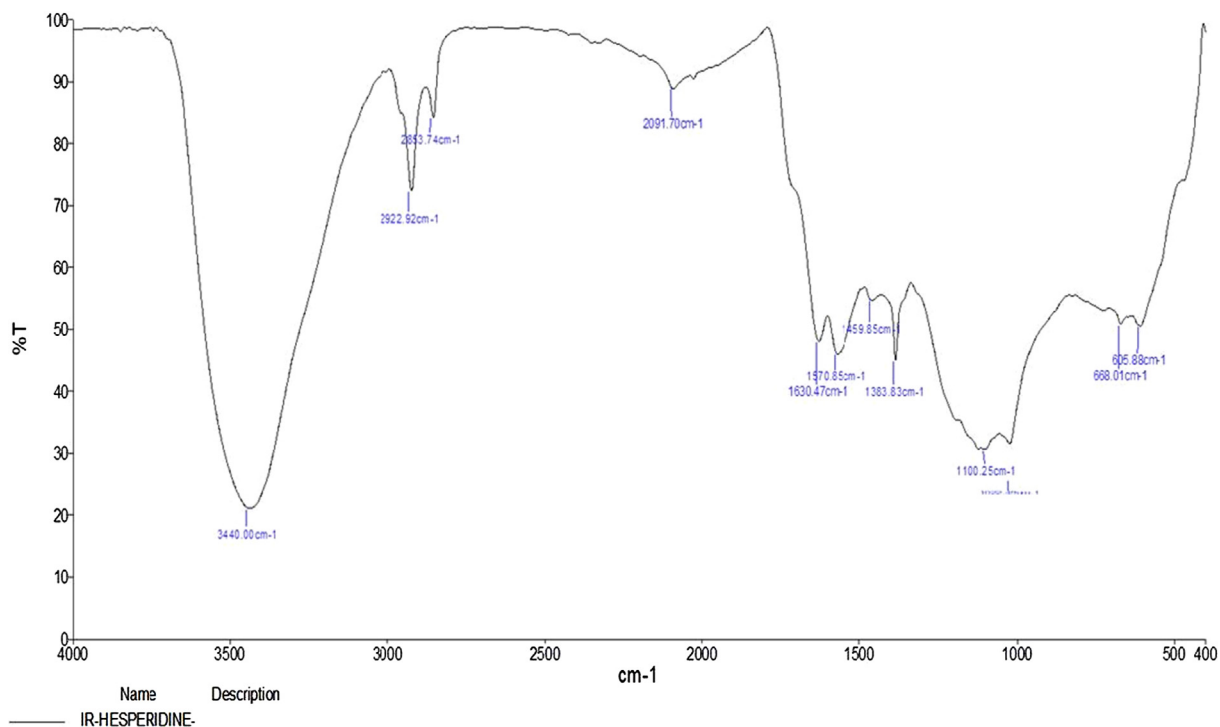

Fig. 3 FTIR spectrum of graphine oxide loaded hesperidin. Hesperidin were responsible for the arrangement of a assortment of nanoparticles. The FTIR range of Hesperidin exemplified numerous absorption peaks assorted from 3440 cm to 1 to 605 cm^{-1}. Fig. 3 shows the representative FT-IR spectra obtained from hesperidin.

a dose of 10 mg/kg b. wt (group IV) displays much reduction ($p < 0.05$) in inflammatory and interleukin markers. This implies that there was no substantial variance in the levels of this proinflammatory cytokine and interleukin between group I and group IV. The same results were observed in hesperidin managed caspase 3 and 9 (Fig. 10).
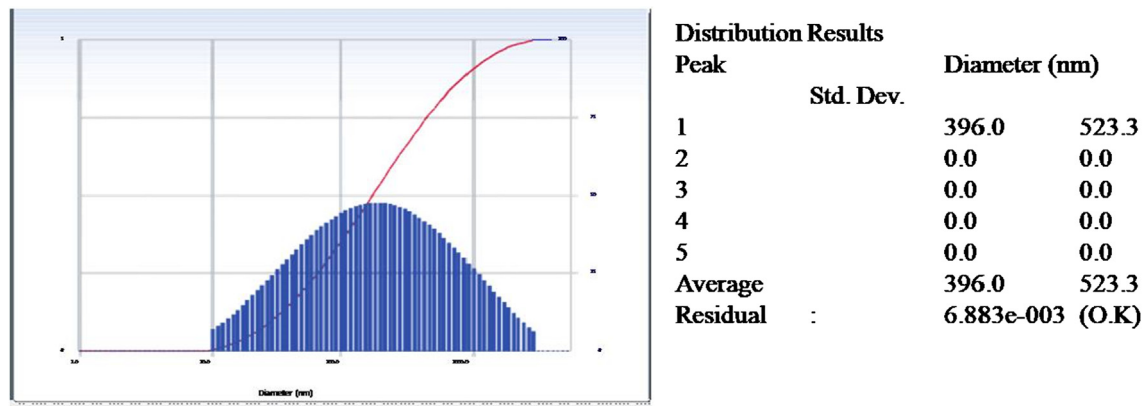
Distribution Results		
Peak		Diameter (nm)
	Std. Dev.	
1		396.0	523.3
2		0.0	0.0
3		0.0	0.0
4		0.0	0.0
5		0.0	0.0
Average		396.0	523.3
Residual :		6.883e-003 (O.K)	

Fig. 4 Intensity Distribution of graphine oxide loaded hesperidin by DLS. DLS measurement of graphine oxide nanosheets at graphine oxide contents 0.2 mol/l. DLS: dynamic light scattering.
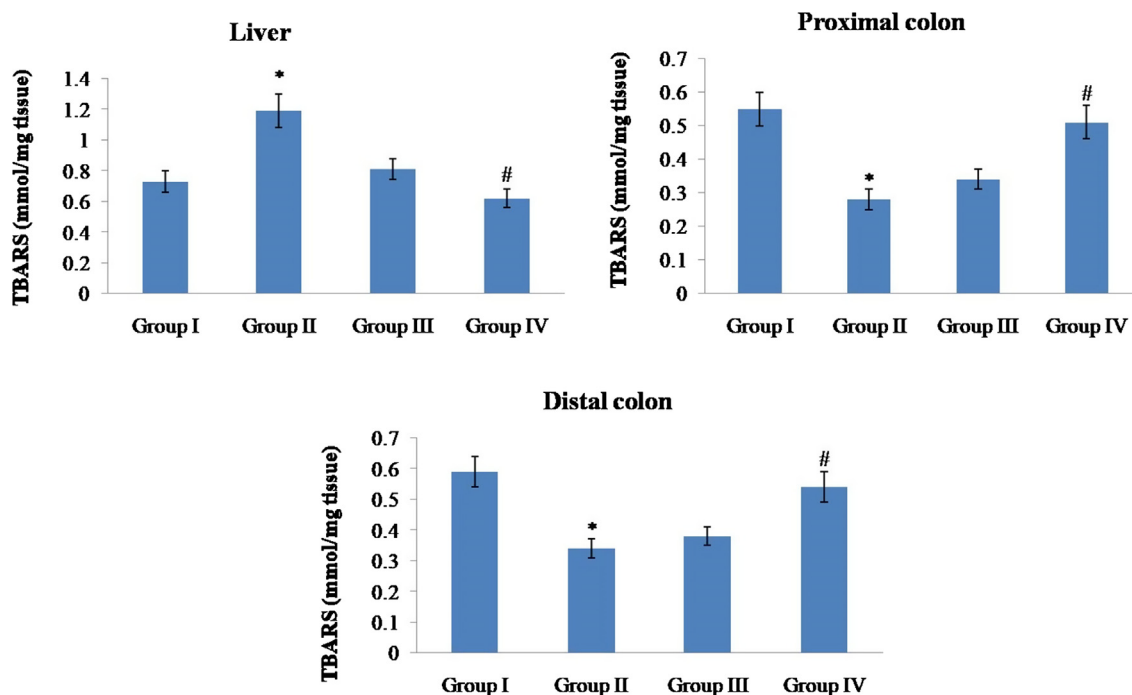

Fig. 5 Effect of hesperidin on thiobarbituric acid reactive substances (TBARS) in the tissues of control and experimental rats. Values are given as mean ± SD for six rats in each group. Values not sharing a common superscript symbol (*,#) differ significantly at P < 0.05 (DMRT).

DMH alone treated exhibited downregulated caspases expressions, at the same time treatment with hesperidin at the doses of (5 and 10 mg/kgb.w) restored or upregulated (p < 0.05) the outcome of caspase 3 and 9. That too hesperidin at 10 mg/kgb.w there is no much substantial difference between group IV and control animals.

3.8. Outcome of hesperidin on COX-2 and iNOS

In DMH alone group II animals the COX-2 and iNOS proteins displayed further positive staining likened to group I (control). In group III hesperidin at dose (5 mg/kg b.wt) the COX-2 and iNOS countenance seemed somewhat diminution in colon tissue related to group II (DMH alone). In group IV hesperidin at a dose of (10 mg/kg b.w) exhibited considerable decline in COX-2 and iNOS protein countenance in colonic tissue as associated to group II (DMH alone). No noteworthy alteration was experiential in staining pattern in group IV as comparable to group I normal rats. This was depicted in Figs. 11 and 12.

3.9. Examination of hesperidin on colon histopathology

Fig. 13 represents the micrograph images of H&E blemished colon mucosal segments of normal and investigational animals. Control (group-I) of colon visualized regular colonic
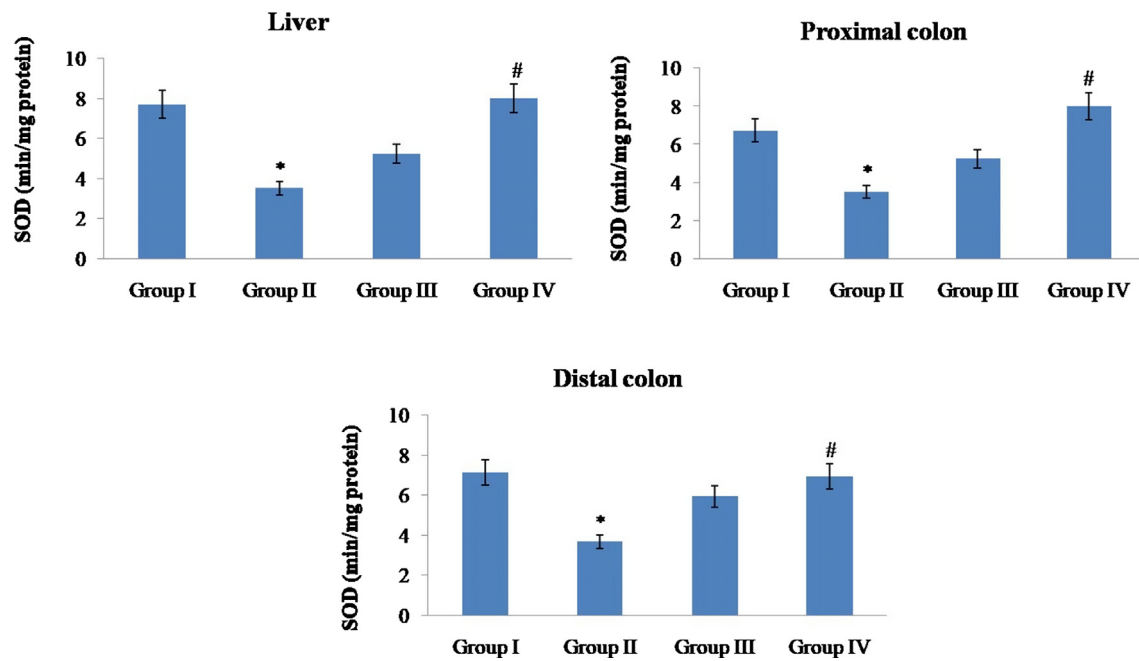
Fig. 6 Effect of hesperidin on superoxide dismutase in the tissues of control and experimental rats. Values are given as mean ± SD for six rats in each group. Values not sharing a common superscript symbol (*, #) differ significantly at P < 0.05 (DMRT).
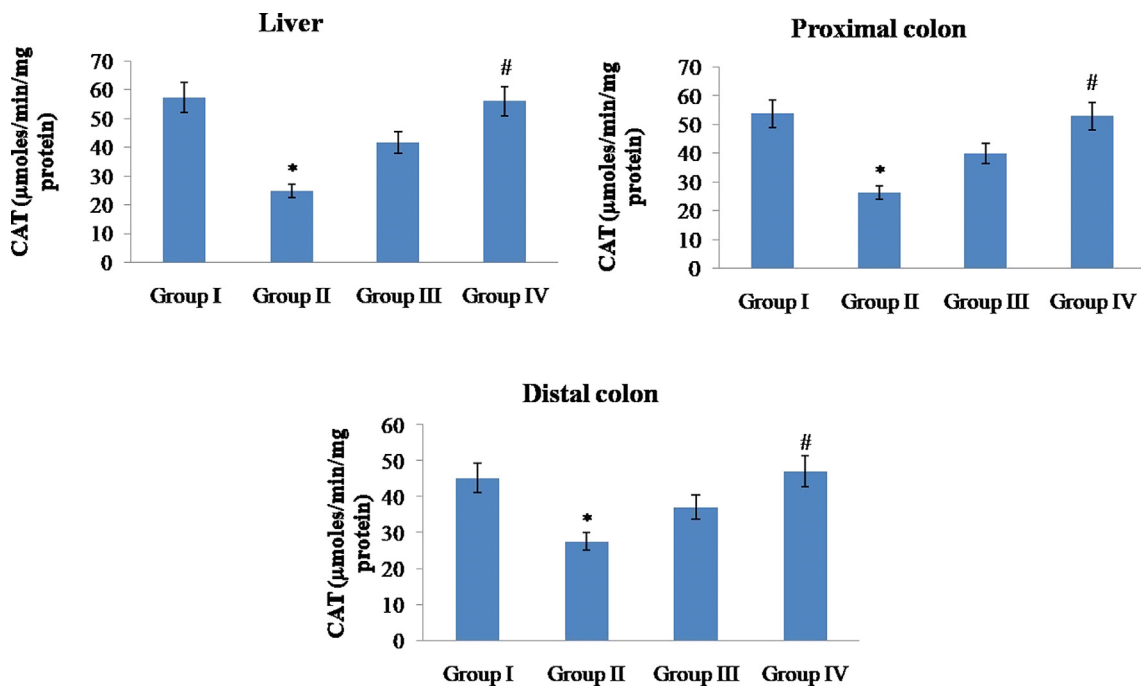

Fig. 7 Effect of hesperidin on catalase in the tissues of control and experimental rats. Values are given as mean ± SD for six rats in each group. Values not sharing a common superscript symbol (*, #) differ significantly at P < 0.05 (DMRT).

construction with consistent mucosal coating (Fig. 9 group I–IV corresponds to A–D). DMH alone animals (group II) of colon illustrate defeat of regular colonic structural design and epithelial veracity, outstanding lymphoid summative which taken together with glands creased by dysplasia cells,

as well as provocative cubicle penetration in mucous and associate mucous stratums (Fig. 13). It is remarkable that colon mucosa of DMH induced animals enhanced through hesperidin at the dose around 5 mg/kg b.w. (III group) depicted close to normal emergeas good colonic construction and
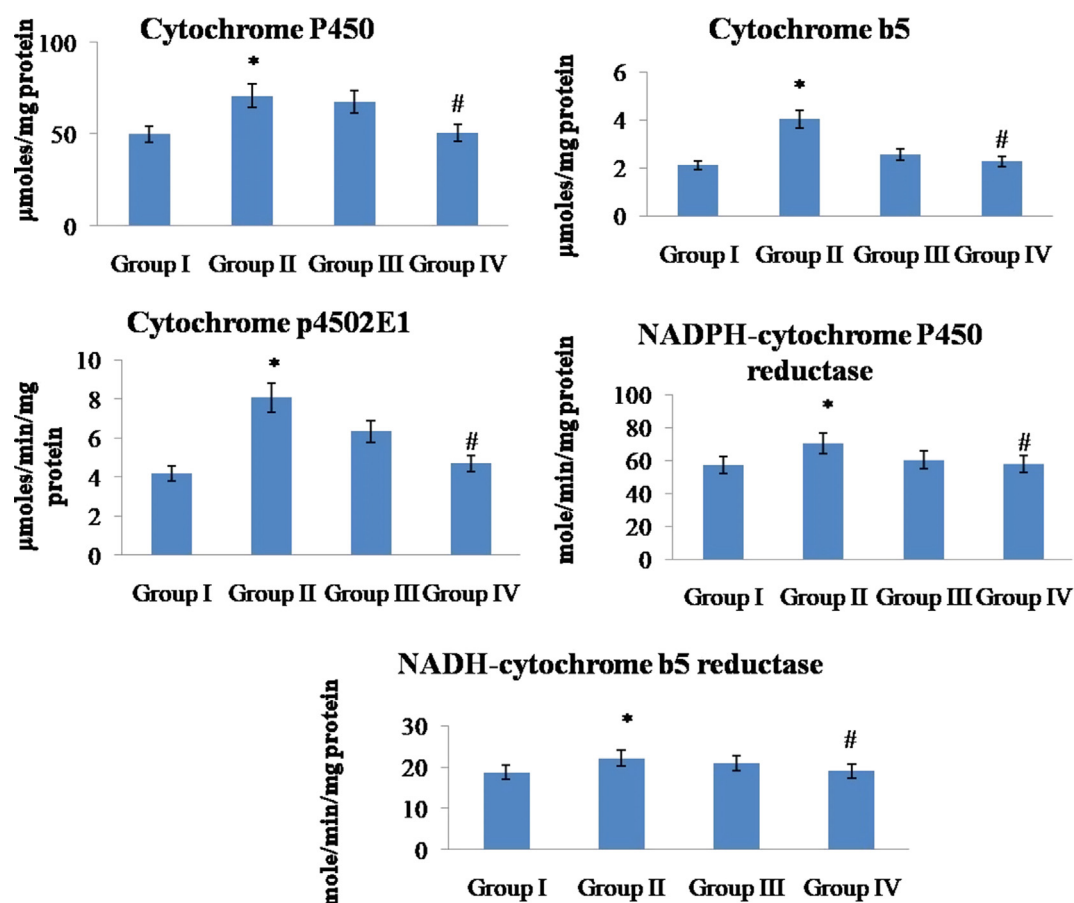
Fig. 8 Effect of hesperidin on phase I enzymes in the liver of control and experimental rats. Values are given as mean ± SD for six rats in each group. Values not sharing a common superscript symbol (*, #) differ significantly at P < 0.05 (DMRT).

hesperidin at 10 mg/kg b.w. (group IV) displayed only modest provocative cell permeate in the colon mucosa.

3.10. Examination of hesperidin on liver histopathology

Fig. 14 signifies the photomontage of same H&E discolored liver segment of control and tentative animals. Group-I animals of colon envisaged standard colonic assembly with reliable liver staining (Fig. 10 (group I–IV corresponds to A–D). DMH alone rats (group II) of colon depicted alteration in the liver distinguished by thrashing of regular structural design, fatty changes of vesicular cells, hyperplasia of Kupffer cell, unstable extent of anaplasia and stirring cell permeation in the porch chord (Fig. 14). And also notable with the intention of colonic mucosa of DMH induced wistars improved through hesperidin at the dosage of 5 mg in group III animals displayed close to regular structural design furthermore hesperidin at the dose of 10 mg in group IV animals demonstrates seditious infiltrate as well abnormal cell growth.

4. Discussion

DMH is a powerful genotoxic carcinogen that is extensively used to persuade colon cancer in rat models (Twelves et al., 2005; Heitman et al., 1983). It fabricates unpaired electrons in the specialized body fluid like blood, liver and bulky bowel in investigational animal sculpts (Weisburger, 1971). The representation that provokes rat colon cancer duplicates human neoplasms in epithelial cells. Current exploration was proficient toward appraising the prospective efficacy of hesperidin in DMH persuaded rat colon cancer. Hesperidin, a citrus flavonoid, stated that it possess numerous biological properties (Trivedi et al., 2011; Parhiz et al., 2015; Bai et al., 2019; Tanaka et al., 2012; Jo et al., 2019).

In current exploration, DMH initiation in rats demonstrates abridged body mass increase and expansion rate, which is comparable to preceding reports (Vinothkumar et al., 2013). The rationale that DMH induced rats depicted condensed body mass and growth speed might be owed to the compacted vigor processing in cancerous circumstances. During agreement through preceding studies, we encompass as well observed absolute occurrence of hypergenesis stalks or polyps in DMH unaided animals in comparable to additional groups. The declined body weight increase, growth tempo and augmented polyps prevalence, in DMH alone administered animals displaying the preliminary phase of colon cancer. Nevertheless, management with hesperidin to DMH induced animals displayed upregulated body mass and development speed, and diminished abnormal stalk occurrence, therefore withdrawing the possessions of DMH.

XRD pattern confirmed the pattern of graphine oxide nanosheets. FTIR spectra revealed the presence of ($=$C$-$H,
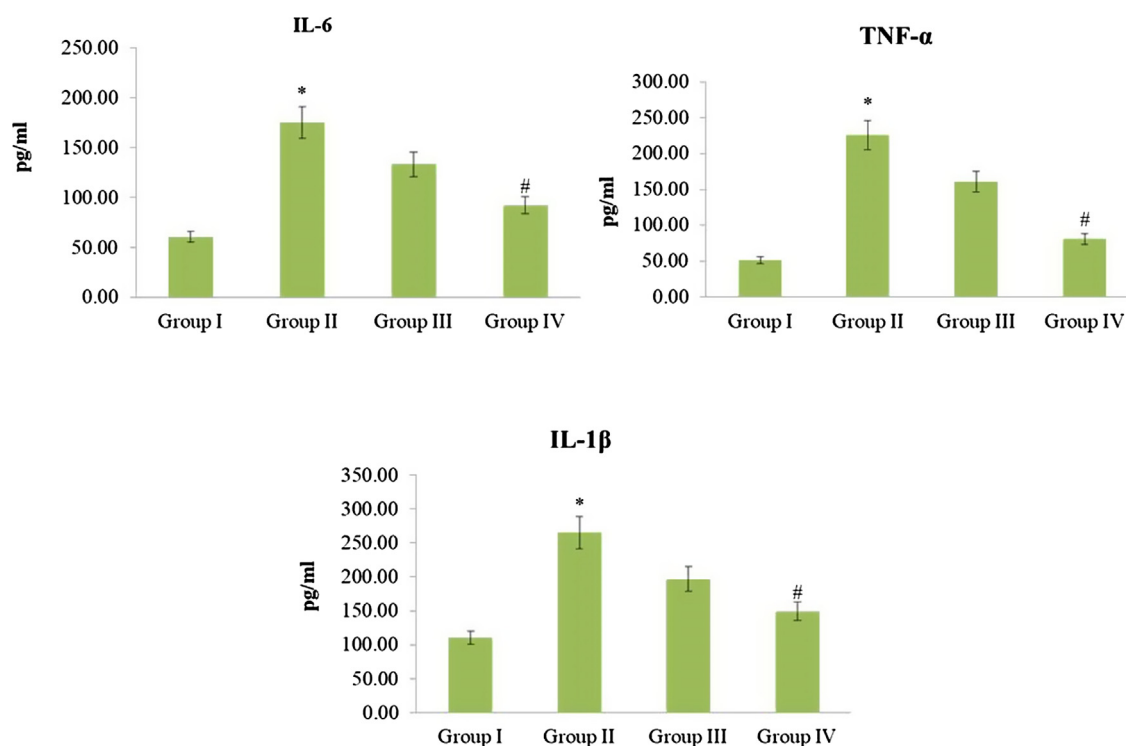
Fig. 9 Effect of Hesperidin on Inflammatory and Interleukins in control and experimental rats. Effect of hesperidin on IL-6, IL- 1β, and TNF-α expression levels in control and experimental groups were analysed by ELISA. The quantification was carryied out by densitometric using image software. The densitometry data symbolize means ± SD from independent experiments. Values are not sharing a common marking (* and #) differ significantly at $P < 0.05$ (One way ANOVA followed by DMRT).
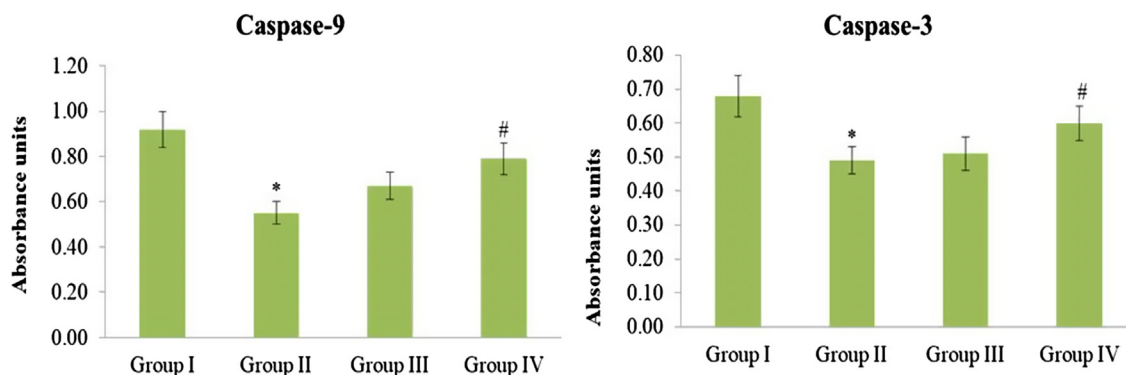

Fig. 10 Effect of Hesperidin on caspase 9 and 3 control and experimental rats. Effect of hesperidin on Caspase-9 and Caspase-3 expression levels in control and experimental groups were analysed by ELISA. The quantification was carried out by densitometric using image software. The densitometry data symbolize means ± SD from independent experiments. Values are not sharing a common marking (* and #) differ significantly at $P < 0.05$ (One way ANOVA followed by DMRT).

C—O, C—H, C═C and OH) functional clusters accredited to the biologically active molecules present in hesperidin. Preceding findings make possible the reduction of graphine oxide from hydrazine during the element expansion and annihilation procedure. Chemical modification of graphene oxide nanosheets in plasma of blood influences their communications among cells (Xiangang et al., 2017). In current study the spectrum achieved to discriminate the boundary among hesperidin and Chloroauric acid has powerful peak at 3440.0 demonstrate different functional groups (OH group, ahead of peaks, few added peaks at 2922 and 2853 were also obtained

which contest with C—H group, C—O group ═C—H group and C═C group.

Previous UV–Vis spectroscopic findings, shows it can be contingent that the visual amalgamation of graphine oxide is conquered by the plasmon peak near 230 nm. The peak resides on two category of conjugative outcome: one is associated to nanometer scale cluster, and another one occurs from connecting functional groups such as C═C, C═O and C—O bonds 9. In which, the decontextualize peaks occurred at obligatory energy array of 284.8–285, 286–287 and 288–289 eV are accredited to the C═C, C—O and O═C oxygen enclosing car-
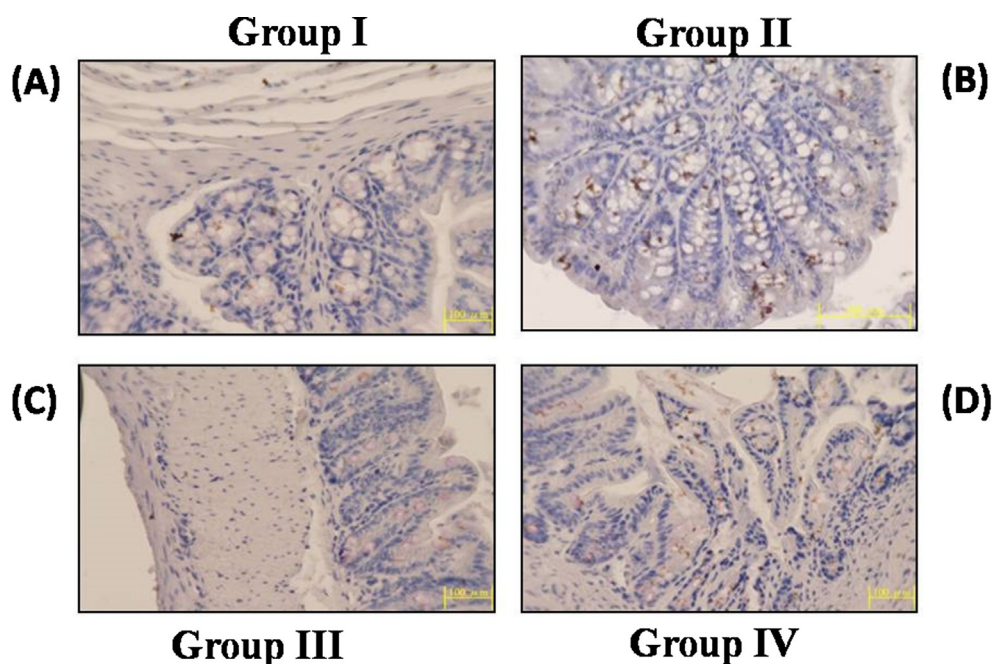
Fig. 11 Effect of Hesperidin on iNOS by immunohistochemistry in control and experimental rats. The iNOS expression of control and experimental animals in each group (20×). A & D iNOS expression in control and hesperidin (10 mg/kg b.w.) administered animals. B. Shows the over expression of iNOS in DMH alone treated. C. Shows the diminished expression of iNOS in DMH + hesperidin (5 mg/kg b.w.) administered animals.
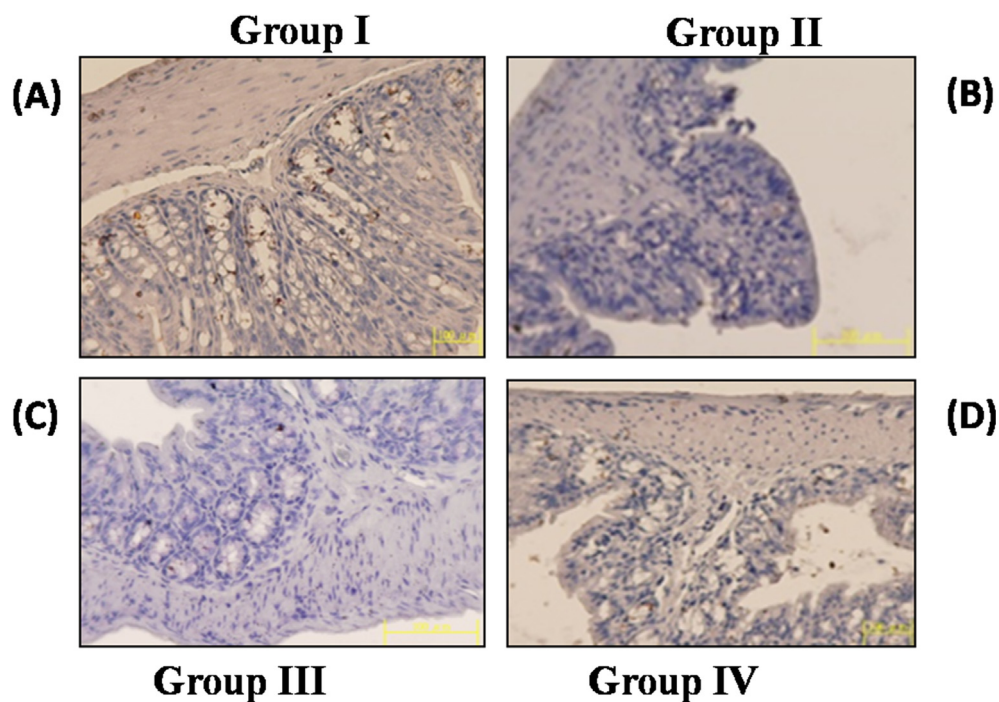

Fig. 12 Effect of Hesperidin on COX-2 by immunohistochemistry in control and experimental rats. The COX-2 expression of control and experimental animals in each group (20×). A & D COX-2 expression in control and hesperidin (10 mg/kg b.w.) administered animals. B. Shows the over expression of COX-2 in DMH alone treated. C. Shows the diminished expression of COX-2 in DMH + hesperidin (5 mg/kg b.w.) administered animals.
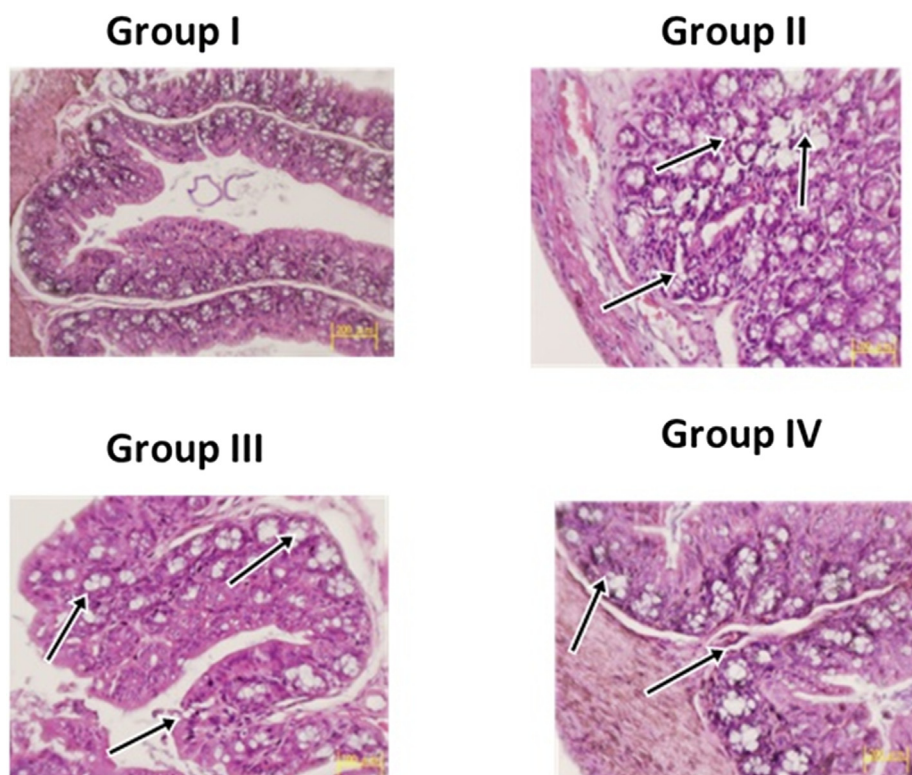
Group I

Group II

Group III

Group IV

Fig. 13 Histopathology of Colon mucosa on control and experimental rats. Histological results of colon mucosa of control and experimental rats. (a and d) control and DMH along with hesperidin (10 mg/kg b.w) rats showing normal & moderate colon mucosa design. DMH (1,2-Dimethylhydrazine) alone rat colonic (group II) displays viewing defeat of epithelial veracity, with expand lumen, important lymphoid summative, seditious cell infiltrate in the mucosal layers. The colonic mucosa of DMH + hesperidin 5 mg/kg body weight (group III) depicts near normal colonic mucosal structural pattern. Histological alterations were pointed out by the arrow marks.

bon bands, correspondingly (Eda et al., 2010; Eda and Chhowalla, 2010; Cai et al., 2008; Akhavan and Ghaderi, 2009). In present study UV–vis spectra confirmed at assorted time break for the rejoinder with solution present in appearance of peak absorbance range at 876.25 nm at the wavelength of 400. The consequent UV–vis spectrum verified from hyaluronic acid attenuation at dissimilar time space is shown in Fig. 1. On refuse of hyaluronic acid for a range of occurrence portrayed a reject in the potency of graphine oxide at 876.25 & 234.15 nm and appearance of band at 876.25 nm.

Furthermore, present study exemplified that DMH alone induced animals improved lipid peroxidation in the liver which coincides with preceding studies (Vinothkumar et al., 2013; Giftson et al., 2010). Lipid peroxidation symbolizes one of the most recurrent responses caused by reactive oxygen species assault resultant in cellular injures intogenetic structures which results in colon tumor. Reactive oxygen species is blameworthy concerned in disease development and molecular process of instigation, endorsement and development in this type of cancer. In current study, animals induced alone with DMH displayed downregulated planes of lipids in colon tissues which might associate among numerous studies that are performed beforehand (Sreedharan et al., 2009; Vinothkumar et al., 2014; Ozen and Korkmaz, 2003; Yu, 1994). Diminished colonic lipid peroxidation experiential in DMH treated animals which might be owed to augmented cell propagation, amplified confrontation and condensed vulnerability of intenting organs to free radical assault.

Conversely introduction of hesperidin to DMH treated rats extraordinarily reinstates almost to the normal range highlight the fact that hesperidin successfully restrains lipid peroxidation. Antioxidant biocatalyst guards' cells aligned with a range of internal and external toxic complexes such as reactive oxygen species (ROS) and carcinogens related to chemicals (Ding and Kaminsky, 2003). CAT and SOD the principal biological defensive enzymes concerned in straight eradication of lethal electron pair acceptor or formation free radicals (Mo et al., 2009), participate a momentous function in hunting ROS. Present study illustrates the abridged actions of antioxidant enzymes in DMH induced animals might be owed to abnormal augment in intensities of reactive oxygen species plus therefore the oxidative strain, combined among propagation of malignant colonnades. GPx, an antioxidant enzyme, which contains selenium, assist the toxic substance removal of hydrogen peroxide and GSH, a chief, sulphur compound with non-protein thiol in many organisms, and execute an innermost position in synchronizing inherent antioxidant shielding mechanisms. Conversely, GR restore GSH commencing corroded glutathione through commencement of GPx in NADPH overwhelming procedure. The diminish in absorption of these internal enzymes in DMH provoked rats, might be frequently owed because of extreme exploitation by cancer cells intended for cellular production on management with hesperidin, considerably augmented the actions that might be accredited to the antioxidant possessions of hesperidin. Liberated groups (hydroxyl) that are in attendance with hesperidin act hydrogen
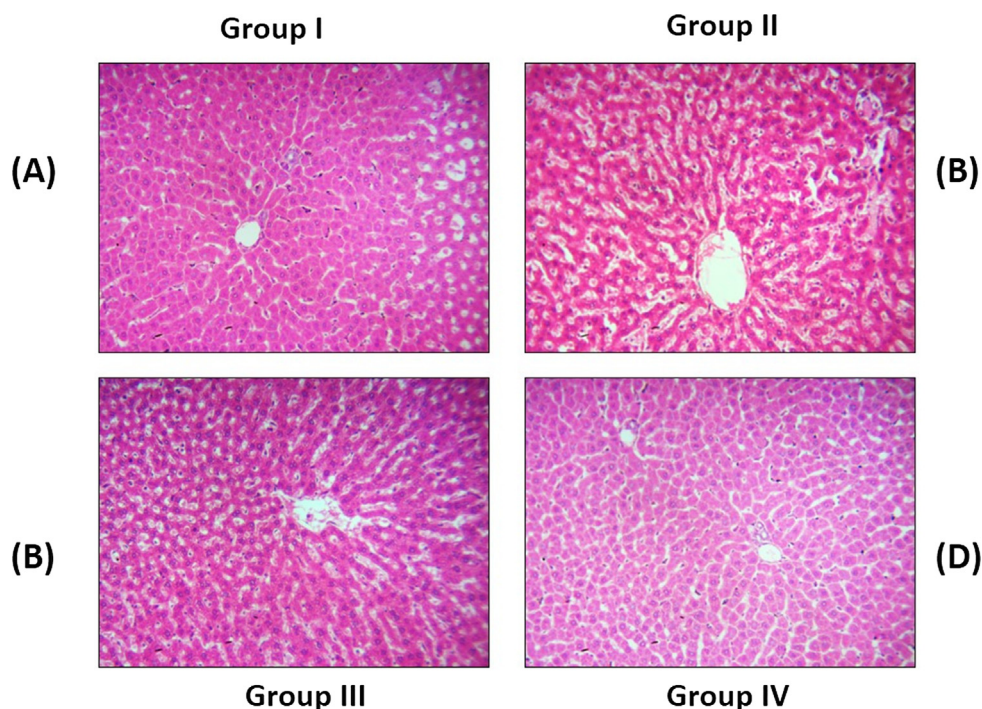
Group I **Group II**

Group III **Group IV**

Fig. 14 Histopathology of Liver on control and experimental rats. Histological results of liver of control and experimental rats [H&E staining]. (a and d) control and DMH along with hesperidin (10 mg/kg body weight) rats showing normal & moderate liver architecture. 1,2-Dimethylhydrazine (DMH) alone rat liver (group II) displays vesicular type of fatty alterations, Kupffer cell hyperplasia, nuclear pleomorphism and provocative cell infiltrate in the portal chord. The liver section of DMH + hesperidin 10 mg/kg b.w. (group III) rat depicted noticeable seditious cell permeate and neoplastic cells. The liver of DMH + hesperidin 5 mg/kg body weight (group IV) showing near normal architecture. Histological alterations were pointed out by the arrow marks.

contributor formulate as significant antioxidant mediator as well as eventually indicate its position in hunting of free radicals.

Enzymes like phase I biotransforming enzymes and cytochrome p450 isozymes, i.e., cytochrome b5, NADPH-cytochrome P450 reductase and NADH-cytochrome b5 reductase are the key enzymes concerned in the establishment of substances that cause cancer (Guengerich, 2005). CYP2E1 anisoetales of CYP450, might accelerates procarcinogens alterations a significant marchin the pattern of formation of adduct DNA provoked via impending cancer causing agents in humans (Murataliev et al., 2004). CPR (NADPH-cytochrome P450 reductase) is accountable for relocating electrons to numerous logically happening electron acceptors, which includes cytochrome-b and cytochrome P450 enzymes also a few inappropriate electron gaining that are frequently used to check enzymatic commotion of NADPH-cytochrome P450 reductase in human liver microsome cells (Murataliev et al., 2004).

In present study, we experiential that a momentous amplification in liver and colonic mucosa phase I enzymes, that might be accredited owing to DMH processing in microsomes of hepatic and cells of epithelial in colon. Ahead of hesperidin management towards DMH induced animals, actions of phase I biological enzymes turn back to in close proximity toregular. Current finding propose with the intention of hesperidin may perform like bifurcate induction, transforming liver enzymes like (Phase I as well II) xenobiotic metabolism enzymes in that

way magnifying detoxification, dropping the development of hasty intercessor and lessening the fabrication of mutation causing agent and cancer causing agents that may be chemical, physical properties or others.

Additionally, our histopathological interpretation exposed assorted series of pathological aberration in the colonic mucosa and hepatic of DMH induced animals. Outcomes were point out that the management with hesperidin downregulates the pathological modification in colon mucosa thus dropping the amount of abnormal cells (dysplastic) in DMH induced experimental animals. In adding up hesperidin efficiently abridged provocative cell permeation, hyperplasia and anaplasia and in hepatic or liver tissues of DMH provoked animals corroborate powerful anti-cancer and hepatoprotective efficiency of hesperidin adjacent to colon cancer. Ultimately preceding work (Vinothkumar et al., 2014) also accounted comparable consequences when the animals were indulged with DMH carcinogen.

5. Conclusion

Current study emphasize confirmation that hesperidin put forth restraining possessions scheduled DMH tempted colonic cancer, that might exist attributed to extraordinary function in toxin removal the cancer causing agents, preserving and balance in pro-oxidant & antioxidant, inflection of the LPO pointers and detoxifying phase enzymes. Graphine oxide nanosheets were enumerated by UV–Vis, XRD, FTIR and

DLS. Biochemical possessions are long-established by the histological outcomes. Among the two (5 and 10) doses of hesperidin, 5 mg/kg b.w. successfully displayed the valuable upshot over DMH provoked colon cancer capable to preferred as optimal dose for investigating the extended tenure possessions of hesperidin.

Declaration of Competing Interest

The authors declared that there is no conflict of interest.

References

Ahmed, K.A., Caudell, J.J., El-Haddad, G., Berglund, A.E., Welsh, E. A., Yue, B., Hoffe, S.E., Naghavi, A.O., Abuodeh, Y.A., Frakes, J. M., Eschrich, S.A., Torres-Roca, J.F., 2016. Radiosensitivity differences between liver metastases based on primary histology suggest implications for clinical outcomes after stereotactic body radiation therapy. Int. J. Radiat. Oncol. Biol. Phys. 95 (5), 1399–1404.

Akhavan, O., Ghaderi, E., 2009. J. Chem. Phys. C 113, 20214.

Al Faraj, A., Shaik, A.S., Al Sayed, B., Halwani, R., Al, J.I., 2016. Specific targeting and non-invasive imaging of breast cancer stem cells using single-walled carbon nanotubes as novel multimodality nanoprobes. Nanomedicine 11 (1), 31–46.

Aranganathan, S., PanneerSelvam, J., Nalini, N., 2009. Hesperetin exerts dose dependent chemopreventive effect against 1,2-dimethyl-hydrazine induced rat colon carcinogenesis. Invest New Drugs 27, 203–213.

Bai, L., Li, X., He, L., et al, 2019. Antidiabetic potential of flavonoids from traditional Chinese medicine: a review. Am. J. Chin. Med. 47 (5), 933–957.

Berkarda, B., Koyuncu, H., Soybir, G., Baykut, F., 1998. Inhibitory effect of hesperidin on tumour initiation and promotion in mouse skin. Res. Exp. Med. 198, 93–99.

Biju, V., 2014. Chemical modifications and bioconjugate reactions of nanomaterials for sensing, imaging, drug delivery and therapy. Chem. Soc. Rev. 43 (3), 744–764.

Bird, R.P., Good, C.K., 2000. The significance of aberrant crypt foci in understanding the pathogenesis of colon cancer. Toxicol. Lett. 15, 395–402.

Cai, W.W., Piner, R.D., Stadermann, F.J., Park, S., Shaibat, M.A., Ishii, Y., Yang, X., Velamakanni, D.X., Stoller, S.J., An, M., Chen, J.H., 2008. Science 321, 1815.

Carlberg, Mannervik, R., 1985. Glutathione reductase. Methods Enzymol. 113, 484–490.

Chattopadhyay, S.N., Pan, N.C., Roy, A.K., Saxena, S., Khan, A., 2013. Development of natural dyed jute fabric with improved colour yield and UV protection characteristics. J. Text. Inst. 104 (8), 808–818.

Chen, Y.C., Shen, S.C., Lin, H.Y., 2003. Rutinoside at C7 attenuates the apoptosis-inducing activity of flavonoids. Biochem. Pharmacol. 66, 1139–1150.

Chen, G.Y., Yang, H.J., Lu, C.H., Chao, Y.C., Hwang, S.M., Chen, C.L., 2012. Simultaneous induction of autophagy and toll-like receptor signaling pathways by graphene oxide. Biomaterials 33, 6559–6569.

Chen, G.Y., Chen, C.L., Tuan, H.Y., Yuan, P.X., Li, K.C., Yang, H. J., 2014. Graphene oxide triggers toll-like receptors/autophagy responses in vitro and inhibits tumor growth in vivo. Adv. Health Mater. 3, 1486–1495.

Ding, X., Kaminsky, L.S., 2003. Human extrahepatic cytochromes P450: function in xenobiotic metabolism and tissue-selective chemical toxicity in the respiratory andgastrointestinal tracts. Annu. Rev. Pharmacol. Toxicol. 43, 149–173.

Eda, G., Chhowalla, M., 2010. Adv. Mater. 22, 2392.

Eda, G., Lin, Y.Y., Mattevi, C., Yamaguchi, H., Chen, H.A., Chen, I. S., Chen, C.-W., Chhowalla, M., 2010. Adv. Mater. 22, 505.

El-Khadragy, M.F., Nabil, H.M., Hassan, B.N., Tohamy, A.A., Waaer, H.F., Yehia, H.M., Alharbi, A.M., Moneim, A.E., 2018. Bone marrow cell therapy on 1,2-dimethylhydrazine (DMH)-induced colon cancer in rats. Cell. Physiol. Biochem. 45 (3), 1072–1083.

Ellman, G.L., 1959. Tissue sulphydryl groups. Arch. Biochem. Biophys. 82, 70–77.

Gan, L., von Moltke, L.L., Trepanier, L.A., Harmatz, J.S., Greenblatt, D.J., 2009. Role of NADPH-cytochrome P450 reductase and cytochrome-b5/NADH-b5 reductase in variability of CYP3A activity in human liver microsomes. Drug Metab. Dispos. 37 (1), 90–96.

Gecer, M.K., Kan, T., Gundogdu, M., Ercisli, S., Ilhan, G., Sagbas, H.I., 2020. Physicochemical characteristics of wild and cultivated apricots (Prunus armeniaca L.) from Aras valley in Turkey. Genet. Resour. Crop Evol. 67, 935–945.

Ghantoji, S.S., Stibich, M., Stachowiak, J., Cantu, S., Adachi, J.A., Raad, I.I., Chemaly, R.F., 2015. Non-inferiority of pulsed xenon UV light versus bleach for reducing environmental Clostridium difficile contamination on high-touch surfaces in Clostridium difficile infection isolation rooms. J. Med. Microbiol. 64 (Pt 2), 191.

Giftson, J.S., Jayanthi, S., Nalini, N., 2010. Chemopreventive efficacy of gallic acid, an antioxidant and anticarcinogenic polyphenol, against 1,2-dimethyl hydrazine induced rat coloncarcinogenesis. Invest New Drugs 28, 251–259.

Globocan, 2012. Estimated Cancer Incidence. Mortality and Prevalence Worldwide in 2012.

Guengerich, F.P., 2005. Reduction of cytochrome b5 by NADPH-cytochrome P450 reductase. Arch Biochem. Biophys. 440, 204–211.

Habig, W.H., Pabst, M.J., Jokoby, W.B., 1974. Glutathione S-transferases the first step inmercapturic acid formation. J. Biol. Chem. 249, 7130–7139.

Heitman, D.W., Grubbs, B.G., Heitman, T.O., Cameron, I.L., 1983. Effects of 1,2- dimethylhydrazine treatment and feeding regimen on rat colonic epithelial cell proliferation. Cancer Res. 43, 1153–1162.

Jiang, Z.Y., Hunt, J.V., Wolff, S.P., 1992. Ferrous ion oxidation in the presence of xylenol orangefor detection of lipid hydroperoxide in low density lipoprotein. Anal Biochem 202, 384–389.

Jo, S.H., Kim, M.E., Cho, J.H., et al, 2019. Hesperetin inhibits neuroinflammation on microglia by suppressing inflammatory cytokines and MAPK pathways. Arch. Pharm. Res. 42 (8), 695–703.

Juan, M.E., Lozano-Mena, G., Sanchez-Gonzalez, M., Planas, J.M., 2019. Reduction of preneoplastic lesions induced by 1,2-dimethyl-hydrazine in rat colon by maslinic acid, a pentacyclic triterpene from Olea europaes L. Molecules 24 (7), 1266.

Kakkar, P.S., Das, B., Viswanathan, P.N., 1984. A modified spectrophotometeric assay forsuperoxide dismutase. Indian J. Biochem. Biophys. 21, 130–132.

Kumar, R., Münstedt, H., 2005. Silver ion release fromantimicrobial polyamide/silver composites. Biomaterials 26 (14), 2081–2088.

Lee, C.J., Wilson, L., Jordan, M.A., Nguyen, V., Tang, J., Smiyun, G., 2010. Hesperidin suppressed proliferations of both human breast cancer and androgen-dependent prostate cancer cells. Phytother. Res. 24, S15–S19.

Liu, C., Chen, C., Yang, F., Li, X., Cheng, L., Song, Y., 2018. Phytic acid improves intestinal mucosal barrier damage and reduces serum levels of proinflammatory cytokines in a 1,2-dimethylhydrazine-induced rat colorectal cancer model. Br J Nutr. 120 (2), 121–130.

Malmsten, M., 2013. Inorganic nanomaterials as delivery systems for proteins, peptides, DNA, and siRNA. Curr. Opin. Colloid Interface Sci. 18 (5), 468–480.

Marsic, N.K., Necemer, M., Veberic, R., Ulrih, N.P., Skrt, M., 2019. Effect of cultivar and fertilization on garlic yield and allicin content in bulbs at harvest and during storage. Turk. J. Agric. For. 43, 414–429.

Megaraj, V., Ding, X., Fang, C., Kovalchuk, N., Zhu, Y., Zhang, Q., 2014. Role of hepatic and intestinal P450 enzymes in the metabolic activation of the colon carcinogen azoxymethane in mice. Chem. Res. Toxicol. 27 (4), 656–662.

Mo, S.L., Liu, Y.H., Duan, W., Wei, M.Q., Kanwar, J.R., Zhou, S.F., 2009. Substrate specificity, regulation, and polymorphism of human cytochrome P450 2B6. Curr. Drug Metab. 10 (7), 730–753.

Mori, M., Hata, K., Yamada, Y., 2005. Significance and role of early lesions in experimental colorectal carcinogenesis. Chem. Biol. Interact. 155, 1–9.

Murataliev, M.B., Feyereisen, R., Walker, F.A., 2004. Electron transfer by diflavin reductases. Biochim. Biophys. Acta. 1698, 1–26.

Ohkawa, H., Ohishi, N., Yagi, K., 1979. Assay for lipid peroxides in animal tissues bythiobarbituric acid reaction. Anal Biochem 95, 351–358.

Omura, T., Sato, R., 1964. The carbon monoxide binding pigment of the liver microsomes. I. Evidence for its hemoprotein nature. J. Biol. Chem. 239, 2370–2378.

Ozen, T., Korkmaz, H., 2003. Modulatory effect of Urtica dioica L. (Urticaceae) leaf extract on biotransformation of enzyme systems, antioxidant enzymes, lactate dehydrogenase andlipid peroxidation in mice. Phytomedicine 10, 405–415.

Parhiz, H., Roohbakhsh, A., Soltani, F., Rezaee, R., Iranshahi, M., 2015. Antioxidant and anti-inflammatory properties of the citrus flavonoids hesperidin and hesperetin: an updated review of their molecular mechanisms and experimental models. Phytother. Res. 29 (3), 323–331.

Patra, S., Mitra, P., Pradhan, S.K., 2011. Preparation of nanodimensional CdS by chemical dipping technique and their characterization. Mater. Res. 14 (1), 17–20.

Ra, K.S., Recknagel, R.O., 1968. Early onset of lipid peroxidation in rat liver after carbontetrachloride administration. Exp. Mol. Pathol. 9, 271–278.

Ramachandran, V., Saravanan, R., 2013. Efficacy of asiatic acid, a pentacyclictriterpene on attenuating the key enzymes activities of carbohydrate metabolism in streptozotocin induced diabetic rats. Phytomedicine 20 (3–4), 230–236.

Rosenberg, D.W., Giardinal, C., Tanaka, T., 2009. Mouse models for the study of colon carcinogenesis. Carcinogenesis 30, 183–196.

Rotruck, J.T., Pope, A.L., Ganther, H.E., Swanson, A.B., Hafeman, D.G., Hoekstra, W., 1973. Selenium: biochemical role as a component of glutathione peroxidase. Science 179 (4073), 588–590.

Rudolph, R.E., Dominitz, J.A., Lampe, J.W., 2005. Risk factors for colorectal cancer in relation to number and size of aberrant crypt foci in humans. Cancer Epidemiol. Biomark. Prev. 14, 605–608.

Sangeetha, N., Viswanathan, P., Balasubramanian, T., Nalini, N., 2012. Colon cancer chemopreventive efficacy of silibinin through perturbation of xenobiotic metabolizing enzymes in experimental rats. Eur. J. Pharmacol. 674 (2–3), 430–438.

Senapati, S., Mahanta, A.K., Kumar, S., Maiti, P., 2018. Controlled drug delivery vehicles for cancer treatment and their performance. Signal Transduct. Target. Therapy 3 (1), 7.

Senica, M., Stampar, F., Mikulic-Petkovsek, M., 2019. Different extraction processes affect the metabolites in blue honeysuckle (Lonicera caerulea L. subsp. edulis) food products. Turk. J. Agric. For. 43, 576–585.

Siddique, A.I., Mani, V., Arivalagan, S., Thomas, N.S., Namasivayam, N., 2017. Asiatic acid attenuates pre-neoplastic lesions, oxidative stress, biotransforming enzymes and histopathological alterations in 1,2-dimethylhydrazine-induced experimental rat colon carcinogenesis. Toxicol. Mech. Methods 27 (2), 136–150.

Siegel, R., DeSantis, C., Jemal, A., 2014. Colorectal cancer statistics. CA Cancer J. Clin. 64, 104–117.

Siegel, R., DeSantis, C., Jemal, A., 2014. Colorectal cancer statistics, 2014. CA: Cancer J. Clin. 64 (2), 104–117.

Sinha, K.A., 1972. Colorimetric assay of catalase. Anal. Biochem. 47, 389–394.

Sreedharan, V., Venkatachalam, K.K., Namasivayam, N., 2009. Effect of morin on tissue lipid peroxidation and antioxidant status in 1, 2-dimethylhydrazine induced experimental colon carcinogenesis. Invest. New Drugs 27 (1), 21.

Sugihara, Y., Zuo, X., Takata, T., Jin, S., Miyauti, M., Isikado, A., Imanaka, H., Tatsuka, M., Qi, G., Shimamoto, F., 2017. Inhibition of DMH–DSS–induced colorectal cancer by liposomal bovine lactoferrin in rats. Oncol. Lett. 14 (5), 5688–5694.

Sun, C., Chen, L., Shen, Z., 2019. Mechanisms of gastrointestinal microflora on drug metabolism in clinical practice. Saudi Pharm. J. 27 (8), 1146–1156.

Tanaka, T., Makita, H., Ohnishi, M., Hirose, Y., Wang, A.J., Mori, H., Satoh, K., Hara, A., Ogawa, H., 1994. Chemoprevention of 4-nitroquinoline 1-oxide-induced oral carcinogenesis by dietary curcumin and hesperidin-Comparison with the protective effect of beta-carotene. Cancer Res. 54, 4653–4659.

Tanaka, T., Tanaka, T., Tanaka, M., Kuno, T., 2012. Cancer chemoprevention by citrus pulp and juices containing high amounts of beta-cryptoxanthin and hesperidin. J. Biomed. Biotechnol. 2012, 516981.

Tensingh Baliah, N., Lega, P.S., 2018. Biosynthesis and characterization of zinc oxide nanoparticles using onion bulb extract. IJTSRD 2, 36–43.

Trivedi, P.P., Kushwaha, S., Tripathi, D.N., Jena, G.B., 2011. Cardioprotective effects of hesperetin against doxorubicin-induced oxidative stress and DNA damage in rat. Cardiovasc. Toxicol. 11 (3), 215–225.

Twelves, C., Wong, A., Nowacki, M.P., et al, 2005. Capecitabine as adjuvant treatment for stage III colon cancer. N. Engl. J. Med. 352, 2696–2704.

Venkatraman, G., Ramya, Shruthilaya, 2012. Nanomedicine: towards development of patient-friendly drug-delivery systems for oncological applications. Int. J. Nanomed. 7, 1043–1060.

Vinothkumar, R., Sudha, M., Viswanathan, P., 2013. Modulating effect of d-carvone on 1,2-dimethylhydrazine-induced pre-neoplastic lesions, oxidative stress and biotransforming enzymes, in an experimental model of rat colon carcinogenesis. CellProlif 46 (6), 705–720.

Vinothkumar, R., Kumar, R.V., Karthikkumar, V., Viswanathan, P., Kabalimoorthy, J., Nalini, N., 2014. Oral supplementation with troxerutin (trihydroxyethylrutin), modulates lipid peroxidation and antioxidant status in 1, 2-dimethylhydrazine-induced rat colon carcinogenesis. Environ. Toxicol. Pharmacol. 37 (1), 174–184.

Watt, K.C., Plopper, C.G., Buckpitt, A.R., 1997. Measurement of cytochrome P4502E1 activity in rat tracheobronchial airways using high-performance liquid chromatography withelectrochemical detection. Anal. Biochem. 248, 26–30.

Weisburger, J.H., 1971. Colon carcinogens: their metabolism and mode of action. Cancer 28, 60–70.

Xiangang, H.U., Dandan, L.I., Li, M.U., 2017. Biotransformation of graphene oxide nanosheets in blood plasma affects their interactions with cells. R. Soc. Chem.

Xiong, S., Xiao, G.W., 2018. Reverting doxorubicin resistance in colon cancer by targeting a key signaling protein, steroid receptor coactivator. Exp. Ther. Med. 15, 3751–3758.

Yu, B.P., 1994. Cellular defenses against damage from reactive oxygen species. Physiol. Rev. 74, 39–162.

Zia-Ul-Haq, M., Ahmad, S., Bukhari, S.A., Amarowicz, R., Ercisli, S., Jaafar, H.Z.E., 2014. Compositional studies and biological activities of some mash bean (Vigna mungo (L.) Hepper) cultivars commonly consumed in Pakistan. Biol. Res. 47, 23.